Association of Glaucoma-Susceptible Genes to Regional Circumpapillary Retinal Nerve Fiber Layer Thickness and Visual Field Defects

Munemitsu Yoshikawa,[1] Hideo Nakanishi,[1] Kenji Yamashiro,[1] Masahiro Miyake,[1,2] Tadamichi Akagi,[1] Norimoto Gotoh,[1,2] Hanako O. Ikeda,[1] Kenji Suda,[1] Hiroshi Yamada,[1] Tomoko Hasegawa,[1] Yuto Iida,[1] Ryo Yamada,[2] Fumihiko Matsuda,[2] and Nagahisa Yoshimura[1]; for the Nagahama Study Group

[1]Department of Ophthalmology and Visual Sciences, Kyoto University Graduate School of Medicine, Kyoto, Japan
[2]Center for Genomic Medicine, Kyoto University Graduate School of Medicine, Kyoto, Japan

Correspondence: Hideo Nakanishi, Department of Ophthalmology and Visual Sciences, Kyoto University Graduate School of Medicine, 54 Kawaharacho, Shogoin, Sakyo-ku, Kyoto 606-8507, Japan; hideon@kuhp.kyoto-u.ac.jp.

See the appendix for the members of the Nagahama Study Group.

Submitted: September 21, 2016
Accepted: April 1, 2017

Citation: Yoshikawa M, Nakanishi H, Yamashiro K, et al.; for the Nagahama Study Group. Association of glaucoma-susceptible genes to regional circumpapillary retinal nerve fiber layer thickness and visual field defects. *Invest Ophthalmol Vis Sci*. 2017;58:2510–2519. DOI:10.1167/iovs.16-20797

Purpose. To examine the associations of the earlier reported glaucoma-related genes to the regional circumpapillary retinal nerve fiber layer thicknesses (cpRNFLTs) and corresponding visual field defects.

Methods. We studied 756 patients with primary open-angle glaucoma (POAG) and 3094 normal controls. Each participant was genotyped for nine single nucleotide polymorphisms (SNPs) of four glaucoma-susceptible genes: the *CDKN2B(AS1)*, *TMCO1*, *CAV1/CAV2*, and *SIX1/SIX6* genes. For the SNPs that were significantly associated with the POAG case–control analyses, the associations of SNP genotypes with the cpRNFLTs of 12 sectors were also analyzed, and then finer assessments were performed using 768 points of the cpRNFLT and corresponding visual field defect sensitivities using case-only subjects.

Results. We confirmed that there was a significant association of the *CDKN2B(AS1)* gene to POAG. For the suggested region-specific associations of these genes with the 12-sectored cpRNFLT, a 768-point cpRNFLT examination showed that rs4977756 near *CDKN2B* had significant signal peaks in the temporal region at 330° to 360° and 0° to 30° (maximum $\beta = 2.92$, $P = 2.9 \times 10^{-5}$ at 351.1° and maximum $\beta = 3.97$, $P = 2.2 \times 10^{-4}$ at 23.4°, respectively). These region-specific signals were validated by the corresponding visual field defect patterns of the paracentral/lower hemifield ($P < 0.05$).

Conclusions. Genetic association analyses using the cpRNFLT with 768 points suggest that the *CDKN2B* gene was associated with paracentral/lower hemifield scotomas. Our regional association analyses on cpRNFLT allow detailed characterization of glaucoma-related genes and should be a new target for genomic studies for glaucoma endophenotypes.

Keywords: glaucoma, retinal nerve fiber layer thickness, CDKN2B, visual field defect, genetics

Glaucoma is a complex vision-threatening disorder that is caused by a combination of genetic and environmental factors.[1–3] It is one of the highest causes of acquired blindness worldwide.[4] Several genome-wide association studies (GWAS) have identified glaucoma susceptibility genes including *CDKN2B(AS1)*,[5] *CAV1/CAV2*,[6] *TMCO1*,[5] and *SIX1/SIX6*.[7] Some of these genes have been confirmed to be associated with glaucoma or related endophenotypes, such as the vertical cup-to-disc ratio (VCDR)[8] and intraocular pressure (IOP).[9]

Glaucoma is characterized by glaucomatous optic neuropathy (GON) with corresponding visual field defects (VFDs) that result from the death of retinal ganglion cells (RGCs) and their axons. Because the VFDs are the most important parameter for GON diagnosis, the relationship between the glaucoma susceptibility genes and the areas of the VFDs has been extensively studied.[10–13] However, visual field tests depend on subjective responses of the glaucoma suspects,[14] and the commonly used standard automated perimetry (SAP) 30-2 program examines less than one-sixth of the whole visual field. Thus, another parameter for GON evaluations is needed to determine the relationship between the glaucoma susceptibility genes and the VFDs.

Recent advances in optical coherence tomography (OCT) have allowed clinicians and researchers to make quantitative evaluations of the circumpapillary retinal nerve fiber layer (cpRNFL) thicknesses. Because the degeneration of the RGCs and their axons usually precedes the depression of visual function,[15] assessments of the cpRNFL thickness (cpRNFLT) should be a better way to detect the early changes of GON with a high degree of reproducibility.[16,17]

Earlier genetic studies evaluated the cpRNFLT by dividing it into four to six sectors, and polymorphisms in the *SIX1/SIX6* gene were found to be significantly associated with cpRNFL thinning in the superior and inferior regions but not in the nasal and temporal regions.[18–20] The question then arises whether analysis of the cpRNFLT with finer sectors might provide more detailed information on the regional changes of the GON.

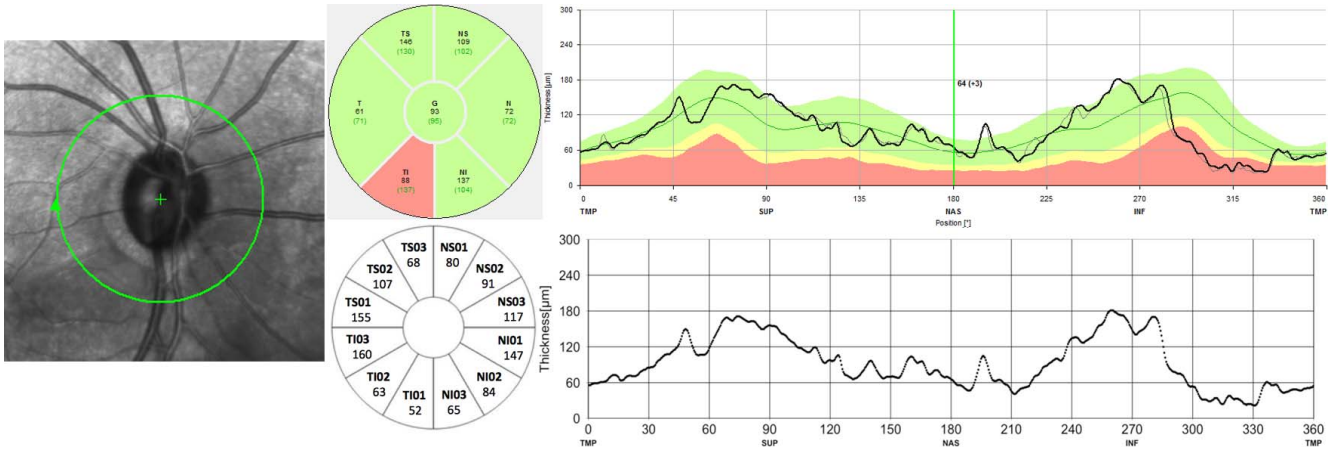

Figure 1. Illustration of the 12-sectored circumpapillary retinal nerve fiber layer thicknesses (cpRNFLT) along the Spectralis (Heidelberg Engineering GmbH) optical coherence tomographic (OCT) circular image. The *upper figures* show the default setting of Spectralis OCT cpRNFLT scanning in 7 sectors, and the *lower figures* show 12 divided sectors of the 12 clock-hour regions composed of 768 cpRNFLT points.

Thus, the purpose of this study was to determine whether the glaucoma susceptibility genes identified in earlier studies were significantly associated with primary open-angle glaucoma (POAG) in Japanese patients. In addition, we examined whether these glaucoma susceptibility genes were significantly associated with alterations of the 12 sectors of the cpRNFLT along the OCT circle scans. The region-specific associations of the genes to GON were further examined at 768 points cpRNFLT and confirmed by the corresponding VFDs.

Methods

Ethics Statement

All procedures used in this cross-sectional observational study adhered to the tenets of the Declaration of Helsinki. The Institutional Review Board and Ethics Committee of Kyoto University Graduate School and the Faculty of Medicine Ethics Committee, the Ad Hoc Review Board of the Nagahama Cohort Project, and the Nagahama Municipal Review Board of Personal Information Protection approved the protocols of this study. All patients were fully informed on the purpose of and procedures to be used in this study, and a written informed consent was obtained.

Study Design

First, we performed a case–control replication analysis on the nine single nucleotide polymorphisms (SNPs) of four glaucoma susceptibility genes, namely, *CDKN2B(AS1)*, *TMCO1*, *CAV1/CAV2*, and *SIX1/SIX6*, in POAG patients and control subjects. Second, we determined whether there were significant associations between the SNP genotypes and any of the 12 sectors of the cpRNFLT in the 360° circumpapillary OCT scan (Fig. 1). We examined these associations in 2-way analyses using the worse eye or both eyes of the case-only groups. For the former analysis, the eyes with the poorer global cpRNFLT were used. For the latter analysis, all repeated measurements of both eyes were used if they met the inclusion and exclusion criteria using generalized estimating equation (GEE) models.[21] For the SNPs that were significantly associated ($P < 4.6 \times 10^{-4}$; 0.05/9 SNPs/12 sectors) and marginally associated ($P < 4.2 \times 10^{-3}$; 0.05/12 sectors) with the cpRNFLT sectors, further assessments of their regional thicknesses were performed for 768 sectors of the cpRNFLT. The associations with the corresponding VFDs were also analyzed to validate these associations.

Subjects

All case subjects were Japanese who were diagnosed with POAG in the Department of Ophthalmology and Visual Sciences of the Kyoto University Hospital. All patients who were examined between January 2008 and October 2014 and consented to have their genomic DNA analyzed were included. The subjects had a complete ophthalmic examination including an objective determination of the refractive error (spherical equivalent), keratometry, IOP measurements with a Goldmann applanation tonometer, slit-lamp biomicroscopy, gonioscopy, indirect ophthalmoscopy, axial length measurements by partial coherence interferometry (IOL Master; Carl Zeiss Meditec, Inc., Dublin, CA, USA), SAP (Humphrey Visual Field Analyzer [HFA]; Carl Zeiss Meditec, Inc.), and cpRNFLT examinations with the Spectralis OCT (Heidelberg Engineering GmbH, Heidelberg, Germany). The exclusion criteria were prior intraocular surgery except for cataract or glaucoma surgery, high myopia with an axial length $\geq$ 26 mm, and presence of other ocular diseases that can influence the visual fields in the studied eye. In the end, 756 patients with POAG were studied.

We used the data of 3094 healthy Japanese volunteers who were enrolled in the Nagahama Prospective Genome Cohort for the Comprehensive Human Bioscience dataset (The Nagahama Study) for the control values. This community-based prospective multi-omics cohort study has been described in detail elsewhere.[22,23] Genome-wide SNP information was available for all subjects. The control subjects also had objectively determined ophthalmic data: the refractive errors, keratometry, fundus photographs, and axial length measurements.[24] We included all participants with axial length < 26 mm because the visual field information was not available for them.

Diagnosis of Primary Open-Angle Glaucoma

POAG was diagnosed by the presence of pathognomonic VFDs that are consistent with GON. GON was diagnosed by the glaucomatous appearance of the optic nerve head, for example, diffuse or localized rim thinning. A glaucomatous VFD was defined as one having the following SAP results: (1) outside the normal limits on glaucoma hemifield tests; (2) three abnormal points with $P < 5\%$ probability of being normal, one

with $P < 1\%$ by pattern deviation; or (3) pattern standard deviation of 5% if the visual field was otherwise normal. An open angle was defined as one not having peripheral anterior synechia or appositional closure of the angle as determined by gonioscopy or anterior segment OCT. The eyes with secondarily elevated IOPs, such as pseudoexfoliation syndrome or uveitis, were excluded.

Circumpapillary Retinal Nerve Fiber Layer Thickness

The Spectralis OCT was used to obtain circular B-scans of 12° diameter centered on the optic disc, that is, a circumpapillary scan, and each B-scan was obtained by averaging 16 images to reduce speckle noise. The cpRNFL thickness was measured as the distance between the inner border of the internal limiting membrane and the outer border of the RNFL semiautomatically with the built-in software.

The RNFL thickness values at 768 points along the 360° OCT circle scan were obtained by the RNFL Export software (Heidelberg Engineering GmbH). All of the acquired images of Spectralis OCT acquisition module version 5 or later (from September 2009) were included. We excluded eyes with extensive peripapillary atrophy (larger than 3.46 mm in diameter or affecting the cpRNFL scans), RNFL schisis, Spectralis quality index < 5 dB, or other segmentation errors of the RNFL in the OCT images. The left-eye data were converted into a right-eye format. We divided the 768-point cpRNFLT values into 12 sectors for the association analyses between the glaucoma-susceptible genes and regional cpRNFLT (Fig. 1).

Visual Field Sensitivity

Reliable visual field tests were those with fixation loss of 20% or less, false-positive rates of 15% or less, and false-negative rates of 15% or less in the 24-2/30-2/10-2 SAP program. For perimetric analyses, all acquired data of the patients were analyzed, but eyes with other ocular diseases or neurologic diseases that can influence visual fields were excluded. We analyzed the visual field sensitivities of paracentral 10° or 24° and the upper and lower hemifields using HFA 10-2 or HFA 24-2/30-2 Swedish Interactive Thresholding Algorithm (SITA) standard. The total deviation values on a decibel scale were converted to 1/Lambert (1/L) scale at all single test positions with the following formula[25]:

$$dB = 10 \times \log_{10}(1/L)$$

Then, the average of 1/L scales at 68 or 52 test points in the HFA 10-2 or 24-2/30-2 programs was analyzed, respectively. Those of the 34 or 26 test points in each hemifield were averaged to evaluate the upper and lower hemifields.

SNP Selection and Genotyping

Previously, nine SNPs for *CDKN2B(AS1)*,[5] three SNPs for *CAV1/CAV2*,[6] two SNPs for *TMCO1*,[5] and one SNP for *SIX1/SIX6*[7] had genome-wide significant associations with POAG in both Asians and Caucasians. We calculated the linkage disequilibrium (LD) between each associated SNP with the HapMap dataset of JPT/CHB using the SNAP software (http://www.broadinstitute.org/mpg/snap/ldsearch.php; in the public domain), and selected representative SNPs from the LD blocks with $R^2 > 0.8$. Minor allelic frequencies (MAF) and reported odds ratio (OR) were also considered to exclude SNPs with insufficient statistical power (<0.8) in Japanese individuals. For *CDKN2B(AS1)*, rs518394, rs10120688, rs10120806, and rs4977756 could represent all nine SNPs with $R^2 > 0.8$ in the Japanese HapMap individuals. Rs10120806 was excluded because a TaqMan probe and primers could not be synthesized. For *CAV1/CAV2*, we selected only the rs1052990 with sufficient MAF and statistical power (>0.8) for the Japanese. For *SIX1/SIX6*, we selected rs33912345 in addition to the reported one SNP (rs10483727), given multiple reports on the functional activity of rs33912345 to cpRNFLT.[18–20] For *TMCO1*, the reported two SNPs were monomorphic in the Japanese, and we selected rs12723198, rs10918271, and rs10918281 from 3 LD blocks with $R^2 > 0.9$ and MAF > 0 in the Japanese HapMap individuals.

Genomic DNA was prepared from peripheral blood using a DNA extraction kit (QuickGene-610L; Fujifilm, Minato, Tokyo, Japan). For the 756 POAG patients, all the SNPs were genotyped using a TaqMan SNP assay with the ABI PRISM 7700 system (Applied Biosystems, Foster City, CA, USA). Sample call rates of ≤0.9 were excluded. For the 3094 controls in the Nagahama study, genotyping and quality control methods were performed as described.[26]

Statistical Analyses

For the assessment of genetic associations with cpRNFLT and VFD using case groups, GEE analyses were applied for a both-eyes model incorporating repeated measurements of the paired-eye data.[21,27–29] Also, linear regression analyses were performed for a worse-eye model. For the case–control replication analyses, logistic regression analyses were performed assuming multiplicative models for the effect of the minor allele with adjustments for age and sex. A P value < 0.05 was considered statistically significant for each SNP in the replication analyses.

For both the GEE analyses and linear regression analyses, the additive effect of the per minor allele was assumed with adjustments for age, sex, and axial length at each visit. We evaluated 12 divided sectors along the OCT circle scan, and Bonferroni corrections were applied to the 9 SNPs and 12 sectors. For the SNPs that were significantly ($P < 4.6 \times 10^{-4}$; 0.05/9 SNPs/12 sectors) or marginally ($P < 4.2 \times 10^{-3}$; 0.05/12 sectors) associated with 12-sectored cpRNFLT, their associations were further evaluated by the analysis of 768 sectors of the cpRNFLT.

For the SNPs that were significantly associated ($P < 4.6 \times 10^{-4}$) with a cpRNFLT in 768 sectors, their associations with corresponding VFD were analyzed to confirm these regional signals. For this purpose, the associations between these SNP variances and visual field sensitivities of 10° or 24° and their upper and lower hemifields were investigated. A P value < 0.05 was considered statistically significant for these analyses.

We used PLINK[30] for the case–control analyses and the R software (http://www.R-project.org/; in the public domain; accessed September 4, 2015) for the other analyses.

Results

There were 740 POAG cases and 2723 controls after standard quality controls. The demographic information on these participants is shown in Table 1.

Case–Control Confirmation Analyses of Association With Glaucoma

The results of the case–control replication analyses of the glaucoma-susceptible SNPs are shown in Table 2. There were significant associations between the presence of POAG and the SNP genotypes of rs518394 and rs4977756 near

Table 1. Demographics of Study Participants

Characteristics	Cases	Controls
Number	740	2723
Age, y*	70.1 ± 11.9	52.5 ± 14.1
Sex, male/female	340/400	878/1845
IOP, mm Hg†	15.97 ± 3.54	NA
Axial length, mm†	24.10 ± 1.12	23.79 ± 1.03
Central corneal thickness, μm†	527.2 ± 33.6	NA
Global cpRNFLT, μm‡	64.5 ± 14.2	NA
HFA 10-2 MD value, dB‡	−10.24 ± 7.71	NA
HFA 24-2/30-2 MD value, dB‡	−8.38 ± 7.63	NA
Visual acuity, logMAR§	0.048 ± 0.331	NA
Spherical equivalent refraction, D†	−1.57 ± 2.71	−1.02 ± 2.17
Follow-up period, y§	7.1 ± 4.2	NA
Anti-glaucoma ophthalmic medication†	1.9 ± 1.2	NA

NA, not applicable; MD, mean deviation; D, diopter.

* These values are shown in mean ± standard deviation. For cases, ages at the time of study inclusion were adopted.

† These values are shown in mean ± standard deviation. For cases, the values at first visit or the nearest ones were adopted and the both-eye data were averaged, if available.

‡ These values are shown in mean ± standard deviation. All acquired data during follow-up were averaged for each patient to calculate each patient value.

§ These values are shown in mean ± standard deviation. The values of the worse eye at the latest visit were adopted.

CDKN2B(AS1) after adjustments for age and sex distribution. The associations of the SNPs of *TMCO1*, *CAV1/CAV2,* and *SIX1/SIX6* with POAG were not significant.

Association of Glaucoma-Susceptible Polymorphisms With Regional cpRNFLT

A total of 4864 images of 680 patients (1208 eyes) were studied. The associations between the nine SNPs of the four glaucoma-susceptible genes and the 12-divided cpRNFLT sectors are shown in Tables 3 and 4. In the both-eye model, the rs4977756 and rs518394 SNPs of *CDKN2B(AS1)* were significantly associated with a regional cpRNFLT (TS [temporal superior] 01; $P = 2.6 \times 10^{-4} < 4.6 \times 10^{-4}$, $\beta = 3.02$; 95% confidence interval [CI]: 1.40–4.64 and TS01; $P = 4.61 \times 10^{-4} < 4.63 \times 10^{-4}$, $\beta = -4.29$; 95% CI: 1.89–6.69, respectively). Two SNPs of *SIX1/SIX6* had marginal associations ($P < 4.2 \times 10^{-3}$) with a regional cpRNFLT. In the worse-eye model, the rs10120688 SNP of *CDKN2B(AS1)* and the two SNPs of *SIX1/SIX6* had marginal associations ($P < 4.2 \times 10^{-3}$) with a regional cpRNFLT. The SNPs of *TMCO1* and *CAV1/CAV2* were not significantly associated with any of the 12-divided cpRNFLT sectors of the two models.

Further assessments of the regional signals were performed using 768 cpRNFLT sectors for these significantly or marginally associated SNPs. The sizes and *P* values of each SNP genotype association with the 768-sector cpRNFLT are shown in Figures 2 and 3. In the both-eye model, rs4977756 near *CDKN2B* had significant signal peaks ($P < 4.6 \times 10^{-4}$) in the temporal and nasal regions at 330° to 360°, 0° to 30°, and 150° to 180° (maximum $\beta = 2.92$ [95% CI: 1.55–4.29], $P = 2.9 \times 10^{-5}$ at 351.1°, maximum $\beta = 3.97$ [95% CI: 1.86–6.07], $P = 2.2 \times 10^{-4}$ at 23.4°, and maximum $\beta = 3.50$ [95% CI: 1.55–5.46], $P = 4.2 \times 10^{-4}$ at 166.4°, respectively). The rs518394 SNP near *CDKN2B(AS1)* had significant signal peaks ($P < 4.6 \times 10^{-4}$) in the temporal region at 330° to 360° and 0° to 30° (maximum $\beta = 3.98$ [95% CI: 1.92–6.04], $P = 1.5 \times 10^{-4}$ at 350.2° and maximum $\beta = 5.31$ [95% CI: 2.35–8.27], $P = 4.4 \times 10^{-4}$ at 22.9°,

Table 2. Genotype Counts of the Glaucoma-Related Single Nucleotide Polymorphisms Among Primary Open-Angle Glaucoma Patients and Controls

CHR	SNP	Gene	Minor Allele*	Other Allele*	Genotype Count		MAF		HWE *P* Value		OR_Nominal† (95% CI)	*P* Value Nominal†	OR_Adjusted‡ (95% CI)	*P* Value Adjusted‡
					Case	Control	Case	Control	Case	Control				
1	rs12723198	*TMCO1*	T	C	85/307/346	251/1171/1301	0.323	0.307	0.18	0.59	1.08 (1.04–1.28)	0.24	1.15 (1.02–1.29)	0.34
1	rs10918271	*TMCO1*	T	C	35/203/501	81/844/1798	0.184	0.185	0.017	0.13	1.12 (0.99–1.26)	0.98	1.10 (0.96–1.26)	0.87
1	rs10918281	*TMCO1*	G	A	110/327/299	362/1269/1092	0.372	0.366	0.19	0.83	1.10 (1.00–1.22)	0.68	1.08 (0.97–1.21)	0.98
7	rs1052990	*CAV1/CAV2*	**G**	T	32/263/445	138/949/1636	0.221	0.225	0.38	0.98	0.98 (0.87–1.10)	0.73	0.99 (0.87–1.14)	0.88
9	rs518394	*CDKN2B-AS1*	C	**G**	13/124/592	57/654/2012	0.104	0.141	0.034	0.65	0.64 (0.55–0.75)	2.3×10^{-4}	0.66 (0.56–0.79)	0.012
9	rs10120688	*CDKN2B-AS1*	G	**A**	70/311/358	341/1221/1161	0.306	0.349	0.84	0.47	0.78 (0.70–0.87)	0.0018	0.80 (0.71–0.90)	0.063
9	rs4977756	*CDKN2B*	G	**A**	37/239/460	184/1039/1500	0.213	0.258	0.41	0.82	0.77 (0.68–0.86)	3.2×10^{-4}	0.75 (0.66–0.86)	0.0020
14	rs33912345	*SIX1/SIX6*	A	**C**	32/243/462	152/1001/1570	0.208	0.240	0.99	0.65	0.91 (0.82–0.99)	0.012	0.89 (0.80–0.99)	0.29
14	rs10483727	*SIX1/SIX6*	C	**T**	32/245/458	156/991/1576	0.211	0.239	0.92	0.99	0.86 (0.76–0.96)	0.021	0.89 (0.78–1.02)	0.35

CHR, chromosome; HWE, Hardy-Weinberg equilibrium.

* Alleles are given relative to the positive strand of NCBI build 37 of the human genome (https://genome.ucsc.edu/cgi-bin/hgGateway, in the public domain). The risk alleles in the previous reports are shown in bold.

† χ^2 test for trend.

‡ Logistic regression analysis assuming multiplicative effect of the per minor allele variant, adjusted for age and sex.

Table 3. Associations of Glaucoma-Related Genes and Circumpapillary Retinal Nerve Fiber Layer Thickness Using Repeated Measurements of Both Eyes in 12 Sectors

CHR	SNP	Gene	TS 01* P†	TS 02* P†	TS 03* P†	NS 01* P†	NS 02* P†	NS 03* P†	NI 01* P†	NI 02* P†	NI 03* P†	TI 01* P†	TI 02* P†	TI 03* P†
1	rs12723198	*TMCO1*	0.16	0.91	0.44	0.90	0.88	0.87	0.26	0.41	0.65	0.84	0.73	0.90
1	rs10918271	*TMCO1*	0.78	0.74	0.19	0.74	0.78	0.43	0.32	0.49	0.66	0.93	0.62	0.61
1	rs10918281	*TMCO1*	0.17	0.60	0.70	0.92	0.67	0.90	0.46	0.30	0.60	0.35	0.58	0.78
7	rs1052990	*CAV1/CAV2*	0.86	0.47	0.66	0.29	0.18	0.89	0.59	0.60	0.47	0.74	0.33	0.79
9	rs518394	*CDKN2B-AS1*	**4.6×10^{-4}**	0.11	0.15	0.90	0.37	0.069	0.061	0.62	0.0051	0.073	**0.0038**	**7.6×10^{-4}**
9	rs10120688	*CDKN2B-AS1*	0.075	0.047	0.26	0.29	0.63	0.13	0.65	0.26	0.020	0.023	0.021	0.046
9	rs4977756	*CDKN2B*	**2.6×10^{-4}**	0.12	0.45	0.69	0.54	0.021	0.12	0.99	0.064	0.83	0.19	**8.9×10^{-4}**
14	rs10483727	*SIX1/SIX6*	0.45	0.25	0.87	0.92	0.23	0.33	0.64	0.86	0.48	**0.0027**	0.34	0.50
14	rs33912345	*SIX1/SIX6*	0.56	0.20	0.83	0.73	0.17	0.41	0.78	0.76	0.35	**0.0015**	0.21	0.64

CHR, chromosome; TS, temporal-superior; NS, nasal-superior; NI, nasal-inferior; TI, temporal-inferior.

* The position of each sector is shown in Figure 1.

† Generalized estimation equation models were applied assuming additive effect for the minor allele variant, adjusted for age, sex, and axial length. Significant ($P < 4.6 \times 10^{-4}$) or suggestive ($P < 4.2 \times 10^{-3}$) associations are shown in bold.

respectively). For the two SNPs of *SIX1/SIX6*, nonsignificant association signals were observed in the inferior region.

In the worse-eye model, rs10120688 near *CDKN2B(AS1)* had significant signal peaks ($P < 4.6 \times 10^{-4}$) between the temporal to superior region at 60° to 90° (maximum $\beta = 10.10$ [95% CI: 5.12–15.08], $P = 8.0 \times 10^{-5}$ at 73.6°). The rs33912345 SNP near *SIX1/SIX6* had significant signal peaks ($P < 4.6 \times 10^{-4}$) in the inferior region at 270° to 300°.

Association of Glaucoma-Susceptible Polymorphisms With Locations of Visual Field Defects

Significant ($P < 4.6 \times 10^{-4}$) associations of the SNPs near *CDKN2B(AS1)* with regional cpRNFLT were confirmed by the severity of VFDs in the corresponding regions. In the both-eye model, 8743 reliable visual field tests of 650 patients (1155 eyes) were included for HFA 24-2/30-2 analyses, whereas 2042 reliable visual field tests of 414 patients (690 eyes) were included for HFA 10-2 analyses. In agreement with the association peaks around 350° and 20° cpRNFLT, a risk allele of rs4977756 near *CDKN2B* had significant associations to both worse paracentral and paracentral lower hemifield scotomas ($P < 0.05$, Table 5).

In the worse-eye model using 650 tests of HFA 24-2/30-2 and 414 tests of HFA 10-2, only a risk allele of rs10120688 near *CDKN2B(AS1)* had a marginal association with the lower hemifield scotoma, and no other significant associations were observed for the other SNPs ($P > 0.05$, Table 6).

Discussion

Our results showed a significant gene–structure relationship between the risk allele of the *CDKN2B(AS1)* gene and the thinner RNFL in the temporal and temporal superior sectors. Further evaluations by finer sectors of the cpRNFLT and VFD led to our finding that the risk allele of rs4977756 was significantly associated with the worse paracentral and paracentral lower hemifield VFDs.

To date, genetic studies on glaucoma have evaluated not only case–control studies on POAG patients but also various endophenotypes such as the IOP, VCDR, disc area, central corneal thickness, VFD,[31,32] and cpRNFLT.[18,20] Among these, the analysis of the cpRNFLT has advantages because of its ability to detect early disease[33,34]; it also has a linear relationship to the GON,[34] is highly reproducible,[34,35] and has a wider examined area than the HFA regions. Although the changes in VCDR represent the progression of GON and glaucoma diagnosis,[36,37] finer analyses using 768-point cpRNFLT would be a better endophenotype for genetic analysis of POAG.

Table 4. Associations of Glaucoma-Related Genes and Circumpapillary Retinal Nerve Fiber Layer Thickness of the Worse Eye in 12 Sectors

CHR	SNP	Gene	TS 01* P†	TS 02* P†	TS 03* P†	NS 01* P†	NS 02* P†	NS 03* P†	NI 01* P†	NI 02* P†	NI 03* P†	TI 01* P†	TI 02* P†	TI 03* P†
1	rs12723198	*TMCO1*	0.29	0.84	0.98	0.74	0.92	1.00	0.77	0.91	0.77	0.75	0.72	0.81
1	rs10918271	*TMCO1*	0.34	0.25	0.43	0.99	0.63	0.50	0.26	0.23	0.52	0.47	0.74	0.86
1	rs10918281	*TMCO1*	0.67	0.97	0.75	0.73	0.86	0.76	0.99	0.79	0.71	0.81	0.80	0.48
7	rs1052990	*CAV1/CAV2*	0.42	0.26	0.16	0.99	0.25	0.26	0.28	0.27	0.62	0.49	0.47	0.65
9	rs518394	*CDKN2B-AS1*	0.0043	0.11	0.53	0.70	0.74	0.48	0.57	0.62	0.0062	0.14	0.058	0.020
9	rs10120688	*CDKN2B-AS1*	0.014	0.0068	**0.0025**	0.14	0.50	0.20	0.90	0.43	0.084	0.37	0.11	0.11
9	rs4977756	*CDKN2B*	0.0068	0.12	0.91	0.68	0.43	0.08	0.49	0.56	0.030	0.96	0.33	0.041
14	rs10483727	*SIX1/SIX6*	0.12	0.27	0.52	0.10	0.06	0.36	0.45	0.37	0.16	**0.0026**	0.24	0.19
14	rs33912345	*SIX1/SIX6*	0.12	0.27	0.55	0.076	0.06	0.40	0.44	0.32	0.11	**0.0014**	0.15	0.28

CHR, chromosome; TS, temporal superior; NS, nasal superior; NI, nasal inferior; TI, temporal inferior.

* The position of each sector is shown in Figure 1.

† Linear regression analyses assuming additive effect for the minor allele variant, adjusted for age, sex, and axial length. Significant ($P < 4.6 \times 10^{-4}$) or suggestive ($P < 4.2 \times 10^{-3}$) associations were shown in bold.

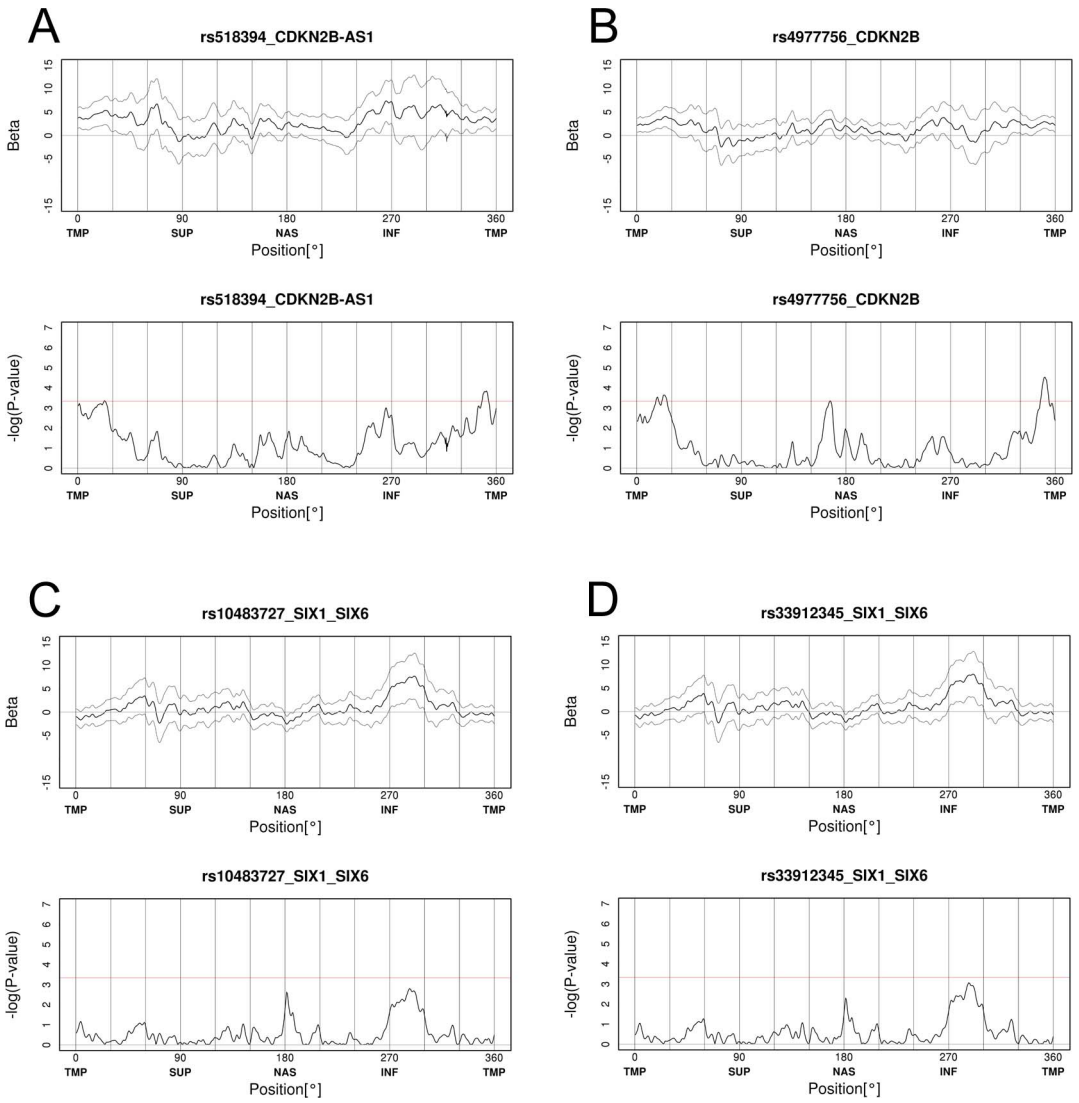

Figure 2. Effect of size, direction, and *P* values of the single nucleotide polymorphism (SNP) genotypes to the 768-point circumpapillary retinal nerve fiber layer thicknesses (cpRNFLT) along with the optical coherence tomographic circle scans in the both-eye model. *First line* shows the effect sizes and 95% confidence intervals based on minor alleles shown in Table 2. The *second line* shows the *P* values plotted in $-\log_{10}$ scale for each SNP. A *red line* shows *P* value of $1 \times 10^{-3.34}$ (= 0.05 / 9 SNPs / 12 sectors = 4.6×10^{-4}). (**A**) Rs518394 near *CDKN2B(AS1)* has suggestive associations with temporal cpRNFLT of 330° to 360° and 0° to 30°. (**B**) Rs4977756 near *CDKN2B* has significant associations with temporal and nasal cpRNFLT at 330° to 360° and 0° to 30° and 150° to 180°, respectively. (**C**, **D**) Rs10483727 and rs33912345 near *SIX1/SIX6* have nonsignificant associations with inferior cpRNFLT of 270° to 300°.

Gene–Structure Relationship and the Corresponding Structure–Function Relationship

Using the both-eye model, the risk allele of rs4977756 near *CDKN2B* was strongly associated with a thinning of the cpRNFLT at around 350° and 20°. According to Hood et al.,[38,39] a thinning in this region should lead to VFDs of the paracentral lower hemifield areas, for the lower and upper hemifield could be separated by around −12° cpRNFL location. Indeed, the risk allele of rs4977756 was significantly associated not only to POAG but also to the severity of paracentral and paracentral lower hemifield VFDs (Table 5). These associations could not be observed when we analyzed paracentral region of the Garway-Heath mapping[40] using HFA 24-2/30-2 (Supplementary Table S1). Thus, it would be of great benefit for such patients with risk alleles of *CDKN2B* to have their visual fields in the central 10° examined more intensively so as not to decrease the quality of vision.[41] On the contrary, using the worse-eye model, the significant genetic association of rs10120688 near *CDKN2B(AS1)* with temporal superior cpRNFLT and that of rs33912345 near *SIX1/SIX6* with inferior cpRNFLT could not be confirmed by the corresponding lower hemifield VFD and upper hemifield VFD, respectively (Table 6; Supplementary Table S2).

Statistical Approach for Repeated Measurement Data

In general, several analytical methods can be applied for repeated measurement data.[42] However, none of them can effectively solve the problems of the randomness and variability of data, the handling of missing or unselected data, and the correlation structure.[43] In addition, some of these models utilized only individuals with complete ophthalmic data at designated time points. It could be inappropriate if the

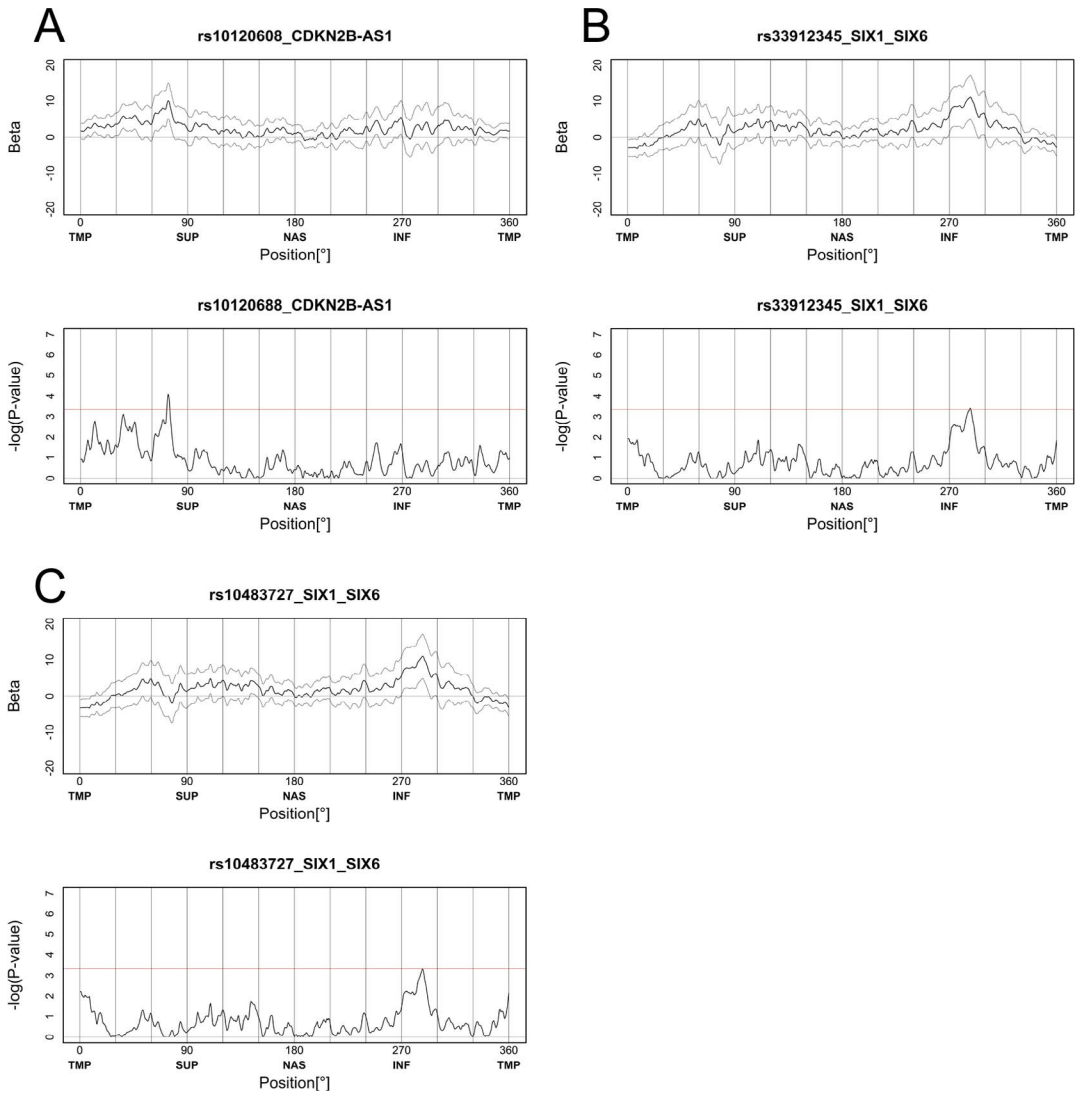

Figure 3. Effect of size, direction, and *P* values of the single nucleotide polymorphism (SNP) genotypes to the 768-point circumpapillary retinal nerve fiber layer thicknesses (cpRNFLT) along with the optical coherence tomographic circle scans in the worse-eye model. *First line* shows the effect sizes and 95% confidence intervals based on minor alleles shown in Table 2. The *second line* shows the *P* values plotted in $-\log_{10}$ scale for each SNP. A *red line* shows *P* value of $1 \times 10^{-3.34}$ ($= 0.05 / 9$ SNPs / 12 sectors $= 4.6 \times 10^{-4}$). (**A**) Rs10120688 near *CDKN2B(AS1)* has significant associations with temporal superior cpRNFLT at 60° to 90°. (**B**) Rs33912345 near *SIX1/SIX6* has significant associations with inferior cpRNFLT at 270° to 300°. (**C**) Rs10483727 near *SIX1/SIX6* have nonsignificant associations with inferior cpRNFLT at 270° to 300°.

mechanism of missing or unselected data depended on the disease-related factors.

To deal with as many of these analytical problems as possible, we used GEE analysis for a both-eye model.[21] Because POAG is a markedly asymmetric disease but the contribution of genetic factors is equal between the two eyes of a patient, analyzing both eyes would lead to a more accurate estimate that excludes various unilateral effects on environment, lifestyle, dominant eye, and traumatic history of the patients. Therefore, we adopted the GEE model as well as the worse-eye model in this study.

Case–Control Replication Study

In the case–control studies, we observed negative associations of the *TMCO1* and *CAV1/CAV2* genes with POAG in Japanese individuals. In fact, the associations of *CAV1/CAV2* to POAG were contradictory in the following replication studies on Japanese patients with POAG[44,45] and on Caucasian patients with POAG.[46,47] For rs1052990 near *CAV1/CAV2* and the three SNPs near *TMCO1*, a type 1 error of 0.05, power of 0.8, and sample/control number of 711/2723, ORs of 1.313 and 1.338 are needed, respectively, to be able to reject the null hypothesis. These ORs are comparable to those in previous reports.[5,6,46] Thus, the association of *CAV1/CAV2* and *TMCO1* to glaucoma is less significant in the Japanese.

There are several limitations to this study. First, earlier studies[48,49] showed that the cpRNFLT was inversely correlated with the axial length. In addition, eyes with longer axial length could be affected by the axial length–related magnification of the OCT images.[50] Thus, we excluded highly myopic eyes and applied statistical adjustment by axial length. Second, in the analyses of cpRNFLT, we included case-only subjects without healthy controls and preperimetric glaucoma patients. If we had included a wider range of disease severity, glaucoma-susceptible SNPs would inevitably be detrimental to the glaucoma-susceptible cpRNFL regions. Thus, the case-only approach would be appropriate. Third, cpRNFLT of the

Table 5. Association Results Between Single Nucleotide Polymorphism Genotypes and Visual Field Sensitivity in the Humphrey Field Analyzer 24-2 and 10-2 Plot Using Repeated Measurements of the Both Eyes

					Hemifield 26 Points						Paracentral Hemifield 34 Points			
			HFA 24-2, 52 Points		Upper		Lower		HFA 10-2, 68 Points		Upper		Lower	
CHR	SNP	Gene	β Adjusted (95% CI)*	*P* Adjusted†	β Adjusted (95% CI)‡	*P* Adjusted†	β Adjusted (95% CI)‡	*P* Adjusted†	β Adjusted (95% CI)*	*P* Adjusted†	β Adjusted (95% CI)‡	*P* Adjusted†	β Adjusted (95% CI)‡	*P* Adjusted†
9	rs518394	*CDKN2B-AS1*	0.02 (−0.03 to 0.07)	0.39	0.03 (−0.03 to 0.09)	0.34	0.02 (−0.03 to 0.06)	0.55	0.04 (−0.00 to 0.08)	0.073	0.03 (−0.02 to 0.08)	0.19	0.05 (−0.00 to 0.09)	0.054
9	rs4977756	*CDKN2B*	0.01 (−0.03 to 0.04)	0.65	0.01 (−0.03 to 0.05)	0.66	0.01 (−0.03 to 0.04)	0.71	0.03 (0.00 to 0.06)	**0.036**	0.02 (−0.02 to 0.05)	0.29	0.05 (0.01 to 0.08)	**0.0050**

CHR, chromosome.

* Effect size on the mean values of 52 or 68 points in HFA 24-2/30-2 or 10-2 total deviation plot. The analyses were performed in 1/Lambert scales.

† Results from generalized estimation equation models, which account for all acquired data of the patients assuming additive effect of the per minor allele variant, adjusted for age at each visit, sex, and axial length. Significant ($P < 0.05$) associations are shown in bold.

‡ Effect size on the mean values of paracentral hemifield 26 or 34 points in HFA 24-2/30-2 or 10-2 total deviation plot. The analyses were performed in 1/Lambert scales.

Table 6. Association Results Between Single Nucleotide Polymorphism Genotypes and Visual Field Sensitivity in the Humphrey Field Analyzer 24-2 and 10-2 Plot of the Worse Eye

					Hemifield 26 Points						Paracentral Hemifield 34 Points			
			HFA 24-2, 52 Points		Upper		Lower		HFA 10-2, 68 Points		Upper		Lower	
CHR	SNP	Gene	β Adjusted (95% CI)*	*P* Adjusted†	β Adjusted (95% CI)‡	*P* Adjusted†	β Adjusted (95% CI)‡	*P* Adjusted†	β Adjusted (95% CI)*	*P* Adjusted†	β Adjusted (95% CI)‡	*P* Adjusted†	β Adjusted (95% CI)‡	*P* Adjusted†
9	rs10120688	*CDKN2B-AS1*	0.05 (0.00 to 0.09)	**0.035**	0.06 (0.00 to 0.11)	**0.039**	0.04 (0.03 to 0.08)	0.077	0.00 (−0.04 to 0.05)	0.88	0.00 (−0.05 to 0.05)	0.93	0.00 (−0.05 to 0.04)	0.86
14	rs33912345	*SIX1/SIX6*	0.02 (−0.03 to 0.07)	0.51	0.03 (−0.02 to 0.07)	0.30	0.01 (−0.05 to 0.07)	0.79	0.01 (−0.04 to 0.05)	0.73	0.02 (−0.03 to 0.08)	0.35	−0.01 (−0.04 to 0.06)	0.72

CHR, chromosome.

* Effect size on the mean values of 52 or 68 points in HFA 24-2/30-2 or 10-2 total deviation plot. The analyses were performed in 1/Lambert scales.

† Linear regression analyses assuming additive effect of the per minor allele variant, adjusted for age at each visit, sex, and axial length. Significant ($P < 0.05$) associations are shown in bold.

‡ Effect size on the mean values of paracentral hemifield 26 or 34 points in HFA 24-2/30-2 or 10-2 total deviation plot. The analyses were performed in 1/Lambert scales.

severely advanced glaucoma patients should be affected by "the floor effect." That is, glaucoma worsening did not correlate with cpRNFLT change in advanced cases. To overcome this limitation, we further confirmed the genetic associations with cpRNFLT by those with VFD, and only consistent results have been reported. In addition, the global cpRNFLT of the worse eye of the patient was normally distributed ($P = 0.28$, Shapiro-Wilk test). Fourth, several glaucoma-susceptible polymorphisms of *CDKN2B(AS1)* showed different associations with cpRNFLT of the temporal region and the temporal superior region. Although we highlighted only rs4977756 showing significant genetic associations with corresponding VFD regions, the associations of rs10120688 with corresponding VFD clusters were marginal. Thus, further studies should be done to disprove these multifaceted gene–structure relationships.

In conclusion, we showed regional associations of *CDKN2B(AS1)* to the temporal cpRNFLT at around 350° and 20° that could be differentiated by analyzing the 768 cpRNFL thicknesses along the OCT circle scan, using large numbers of case-only POAG patients. These cpRNFL regional associations of glaucoma-related genes led to the finding that the *CDKN2B* gene was associated with paracentral and paracentral lower hemifield scotomas. The cpRNFLT with such fineness would be a better endophenotype for genetic analysis of POAG, and it enabled us to determine the effects of glaucoma-related genes on the region-specific RNFLT.

Acknowledgments

The authors thank Hatsue Hamanaka (Kyoto University Graduate School of Medicine, Kyoto, Japan), COA, for her invaluable technical assistance.

Supported in part by the Innovative Techno-Hub for Integrated Medical Bio-Imaging of the Project for Developing Innovation Systems, from the Ministry of Education, Culture, Sports, Science and Technology (MEXT), Japan. This study was also supported in part by a Grant-in-Aid for scientific research (No. 24592624) from the Japan Society for the Promotion of Science, Tokyo, and the Japan National Society for the Prevention of Blindness, Tokyo, Japan.

Disclosure: **M. Yoshikawa**, None; **H. Nakanishi**, None; **K. Yamashiro**, None; **M. Miyake**, None; **T. Akagi**, None; **N. Gotoh**, None; **H.O. Ikeda**, None; **K. Suda**, None; **H. Yamada**, None; **T. Hasegawa**, None; **Y. Iida**, None; **R. Yamada**, None; **F. Matsuda**, None; **N. Yoshimura**, Topcon Corporation (F), Nidek (F), Canon (F)

References

1. Tielsch JM, Katz J, Sommer A, Quigley HA, Javitt JC. Family history and risk of primary open angle glaucoma. The Baltimore Eye Survey. *Arch Ophthalmol*. 1994;112:69–73.
2. Van Koolwijk LM, Ramdas WD, Ikram MK, et al. Common genetic determinants of intraocular pressure and primary open-angle glaucoma. *PLoS Genet*. 2012;8:e1002611.
3. Wiggs JL. Genetic etiologies of glaucoma. *Arch Ophthalmol*. 2007;125:30–37.
4. Tham YC, Li X, Wong TY, Quigley HA, Aung T, Cheng CY. Global prevalence of glaucoma and projections of glaucoma burden through 2040: a systematic review and meta-analysis. *Ophthalmology*. 2014;121:2081–2090.
5. Burdon KP, Macgregor S, Hewitt AW, et al. Genome-wide association study identifies susceptibility loci for open angle glaucoma at TMCO1 and CDKN2B-AS1. *Nat Genet*. 2011;43:574–578.
6. Thorleifsson G, Walters GB, Hewitt AW, et al. Common variants near CAV1 and CAV2 are associated with primary open-angle glaucoma. *Nat Genet*. 2010;42:906–909.
7. Wiggs JL, Yaspan BL, Hauser MA, et al. Common variants at 9p21 and 8q22 are associated with increased susceptibility to optic nerve degeneration in glaucoma. *PLoS Genet*. 2012;8:e1002654.
8. Springelkamp H, Höhn R, Mishra A, et al. Meta-analysis of genome-wide association studies identifies novel loci that influence cupping and the glaucomatous process. *Nat Commun*. 2014;5:4883.
9. Hysi PG, Cheng CY, Springelkamp H, et al. Genome-wide analysis of multi-ancestry cohorts identifies new loci influencing intraocular pressure and susceptibility to glaucoma. *Nat Genet*. 2014;46:1126–1130.
10. Loomis SJ, Kang JH, Weinreb RN, et al. Association of CAV1/CAV2 genomic variants with primary open-angle glaucoma overall and by gender and pattern of visual field loss. *Ophthalmology*. 2014;121:508–516.
11. Buys ES, Ko YC, Alt C, et al. Soluble guanylate cyclase α1-deficient mice: a novel murine model for primary open angle glaucoma. *PLoS One*. 2013;8:e60156.
12. Wiggs JL, Hewitt AW, Fan BJ, et al. The p53 codon 72 PRO/PRO genotype may be associated with initial central visual field defects in caucasians with primary open angle glaucoma. *PLoS One*. 2012;7:e45613.
13. Pasquale LR, Loomis SJ, Kang JH, et al. CDKN2B-AS1 genotype-glaucoma feature correlations in primary open-angle glaucoma patients from the United States. *Am J Ophthalmol*. 2013;155:342–353.e5.
14. Junoy Montolio FG, Wesselink C, Gordijn M, Jansonius NM. Factors that influence standard automated perimetry test results in glaucoma: test reliability, technician experience, time of day, and season. *Invest Ophthalmol Vis Sci*. 2012;53:7010–7017.
15. Sommer A, Katz J, Quigley HA, et al. Clinically detectable nerve fiber atrophy precedes the onset of glaucomatous field loss. *Arch Ophthalmol*. 1991;109:77–83.
16. Miki A, Medeiros FA, Weinreb RN, et al. Rates of retinal nerve fiber layer thinning in glaucoma suspect eyes. *Ophthalmology*. 2014;121:1350–1358.
17. Pierro L, Gagliardi M, Iuliano L, Ambrosi A, Bandello F. Retinal nerve fiber layer thickness reproducibility using seven different OCT instruments. *Invest Ophthalmol Vis Sci*. 2012;53:5912–5920.
18. Cheng CY, Allingham RR, Aung T, et al. Association of common SIX6 polymorphisms with peripapillary retinal nerve fiber layer thickness: the Singapore Chinese Eye Study. *Invest Ophthalmol Vis Sci*. 2015;56:478–483.
19. Carnes MU, Liu YP, Allingham RR, et al. Discovery and functional annotation of SIX6 variants in primary open-angle glaucoma. *PLoS Genet*. 2014;10:e1004372.
20. Kuo JZ, Zangwill LM, Medeiros FA, et al. Quantitative trait locus analysis of SIX1-SIX6 with retinal nerve fiber layer thickness in individuals of European descent. *Am J Ophthalmol*. 2015;160:123–130.e1.
21. Liang KY, Zeger SL. Longitudinal data analysis using generalized linear models. *Biometrika*. 1986;73:13–22.
22. Yoshimura K, Nakayama T, Sekine A, et al. B-type natriuretic peptide as an independent correlate of nocturnal voiding in Japanese women. *Neurourol Urodyn*. 2012;31:1266–1271.
23. Terao C, Bayoumi N, McKenzie CA, et al. Quantitative variation in plasma angiotensin-I converting enzyme activity shows allelic heterogeneity in the ABO blood group locus. *Ann Hum Genet*. 2013;77:465–471.
24. Nakata I, Yamashiro K, Nakanishi H, et al. Prevalence and characteristics of age-related macular degeneration in the Japanese population: the Nagahama study. *Am J Ophthalmol*. 2013;156:1002–1009.e2.
25. Garway-Heath DF, Caprioli J, Fitzke FW, et al. Scaling the hill of vision: the physiological relationship between light sensitivity

and ganglion cell numbers. *Invest Ophthalmol Vis Sci*. 2000; 41:1774–1782.

26. Oishi M, Yamashiro K, Miyake M, et al. Association between ZIC2, RASGRF1, and SHISA6 genes and high myopia in Japanese subjects. *Invest Ophthalmol Vis Sci*. 2013;54:7492–7497.
27. Fan Q, Teo YY, Saw SM. Application of advanced statistics in ophthalmology. *Invest Ophthalmol Vis Sci*. 2011;52:6059–6065.
28. Xu X, Byles J, Shi Z, McElduff P, Hall J. Dietary pattern transitions, and the associations with BMI, waist circumference, weight and hypertension in a 7-year follow-up among the older Chinese population: a longitudinal study. *BMC Public Health*. 2016;16:743.
29. Lee J, Choi JY. Texas hospitals with higher health information technology expenditures have higher revenue: a longitudinal data analysis using a generalized estimating equation model. *BMC Health Serv Res*. 2016;16:117.
30. Purcell S, Neale B, Todd-Brown K, et al. PLINK: a tool set for whole-genome association and population-based linkage analyses. *Am J Hum Genet*. 2007;81:559–575.
31. Chen Y, Hughes G, Chen X, et al. Genetic variants associated with different risks for high tension glaucoma and normal tension glaucoma in a Chinese population. *Invest Ophthalmol Vis Sci*. 2015;56:2595–2600.
32. Burdon KP, Crawford A, Casson RJ, et al. Glaucoma risk alleles at CDKN2B-AS1 are associated with lower intraocular pressure, normal-tension glaucoma, and advanced glaucoma. *Ophthalmology*. 2012;119:1539–1545.
33. Banegas SA, Antón A, Morilla A, et al. Evaluation of the retinal nerve fiber layer thickness, the mean deviation, and the visual field index in progressive glaucoma. *J Glaucoma*. 2016;25: e229–e235.
34. Grewal DS, Tanna AP. Diagnosis of glaucoma and detection of glaucoma progression using spectral domain optical coherence tomography. *Curr Opin Ophthalmol*. 2013;24:150–161.
35. Leung CK, Yu M, Weinreb RN, Lai G, Xu G, Lam DS. Retinal nerve fiber layer imaging with spectral-domain optical coherence tomography: patterns of retinal nerve fiber layer progression. *Ophthalmology*. 2012;119:1858–1866.
36. Foster PJ, Buhrmann R, Quigley HA, Johnson GJ. The definition and classification of glaucoma in prevalence surveys. *Br J Ophthalmol*. 2002;86:238–242.
37. Wolfs RC, Borger PH, Ramrattan RS, et al. Changing views on open-angle glaucoma: definitions and prevalences–The Rotterdam Study. *Invest Ophthalmol Vis Sci*. 2000;41:3309–3321.
38. Hood DC, Raza AS. On improving the use of OCT imaging for detecting glaucomatous damage. *Br J Ophthalmol*. 2014; 98(suppl 2):ii1–ii9.
39. Hood DC, Raza AS, de Moraes CG, Liebmann JM, Ritch R. Glaucomatous damage of the macula. *Prog Retin Eye Res*. 2013;32:1–21.
40. Garway-Heath DF, Poinoosawmy D, Fitzke FW, Hitchings RA. Mapping the visual field to the optic disc in normal tension glaucoma eyes. *Ophthalmology*. 2000;107:1809–1815.
41. Sawada H, Yoshino T, Fukuchi T, Abe H. Assessment of the vision-specific quality of life using clustered visual field in glaucoma patients. *J Glaucoma*. 2014;23:81–87.
42. Verbeke G, Molenberghs G. *Linear Mixed Models for Longitudinal Data*. 2nd ed. New York, NY: Springer; 2000: 19–30.
43. Gewandter JS, McDrmott MP, McKeown A, et al. Reporting of missing data and methods used to accommodate them in recent analgesic clinical trials: ACTTION systematic review and recommendations. *Pain*. 2014;155:1871–1877.
44. Osman W, Low SK, Takahashi A, Kubo M, Nakamura Y. A genome-wide association study in the Japanese population confirms 9p21 and 14q23 as susceptibility loci for primary open angle glaucoma. *Hum Mol Genet*. 2012;21:2836–2842.
45. Kato T, Meguro A, Nomura E, et al. Association study of genetic variants on chromosome 7q31 with susceptibility to normal tension glaucoma in a Japanese population. *Eye (Lond)*. 2013;27:979–983.
46. Wiggs JL, Kang JH, Yaspan BL, et al. Common variants near CAV1 and CAV2 are associated with primary open-angle glaucoma in Caucasians from the USA. *Hum Mol Genet*. 2011; 20:4707–4713.
47. Kuehn MH, Wang K, Roos B, et al. Chromosome 7q31 POAG locus: ocular expression of caveolins and lack of association with POAG in a US cohort. *Mol Vis*. 2011;17:430–435.
48. Savini G, Barboni P, Parisi V, Carbonelli M. The influence of axial length on retinal nerve fibre layer thickness and optic-disc size measurements by spectral-domain OCT. *Br J Ophthalmol*. 2012;96:57–61.
49. Nowroozizadeh S, Cirineo N, Amini N, et al. Influence of correction of ocular magnification on spectral-domain OCT retinal nerve fiber layer measurement variability and performance. *Invest Ophthalmol Vis Sci*. 2014;55:3439–3446.
50. Hirasawa K, Shoji N, Yoshii Y, Haraguchi S. Determination of axial length requiring adjustment of measured circumpapillary retinal nerve fiber layer thickness for ocular magnification. *PLoS One*. 2014;9:e107553.

Appendix

The Nagahama Study Group

The following investigators were core members of the Nagahama Study Group: Takeo Nakayama (Department of Health Informatics, Kyoto University School of Public Health, Kyoto, Japan); Akihiro Sekine (Center for Genomic Medicine, Graduate School of Medicine, Kyoto University, Kyoto, Japan); Shinji Kosugi (Department of Medical Ethics, Kyoto University School of Public Health, Kyoto, Japan); Takahisa Kawaguchi (Center for Genomic Medicine, Graduate School of Medicine, Kyoto University, Kyoto, Japan); Ryo Yamada (Center for Genomic Medicine, Graduate School of Medicine, Kyoto University, Kyoto, Japan); and Yasuharu Tabara (Center for Genomic Medicine, Graduate School of Medicine, Kyoto University, Kyoto, Japan).

Investigative Ophthalmology & Visual Science